CWE-8
June 7-11, 2026
London, ON, Canada

Assessment of an Automatic Mesh Convergence Workflow applied to a Neutral Atmospheric Boundary Layer in Complex Environment

Paul Launay[a,b], Pierre Bénard[c], Lauris Joubert[b], Béatrice Patte-Rouland[a], Léa Voivenel[d]

[a]Univ Rouen Normandie, INSA Rouen Normandie, CNRS, CORIA UMR 6614, F-76000 Rouen, France; paul.launay@coria.fr, beatrice.patte-rouland@univ-rouen.fr
[b]INERIS, French National Institute for Industrial Environment and Risks, 60550 Verneuil-en-Halatte, France; lauris.joubert@ineris.fr
[c]INSA Rouen Normandie, Univ Rouen Normandie, CNRS, Normandie Univ, CORIA UMR 6614, F-76000 Rouen, France; pierre.benard@coria.fr
[d]CNRS, Univ Rouen Normandie, INSA Rouen Normandie, CORIA UMR 6614, F-76000 Rouen, France; voivenel@coria.fr

Summary

An automated mesh convergence workflow for large-eddy simulation (LES) is assessed for a truly neutral turbulent flow around an isolated obstacle. The objectives are to automatically obtain a mesh adapted to a complex flow and quantify the errors induced by spatial discretization. The workflow relies on two criteria designed to assess grid independence of the mean flow field and resolution of turbulent structures by the LES subgrid-scale (SGS) model. A coarse mesh subjected to this automated convergence process is compared to a static mesh, designed according to best practices and guidelines. Both meshes produce results that are consistent with experimental data. However, convergence criteria values appear not restrictive enough to accurately resolve the flow structures near the obstacle surface, and in its wake. Nevertheless, it yields satisfactory results while using fewer elements and requiring lower computational cost. These findings highlight the potential of this workflow for complex atmospheric flows.

Keywords: *mesh convergence, LES, atmospheric flow, complex environment*

1 INTRODUCTION

Atmospheric boundary layer flows are characterized by high Reynolds numbers and a wide range of spatial and temporal scales. In numerical simulations, these scales cannot be resolved using a RANS formulation but can be captured by LES (Tominaga, 2024), which explains the increasing use of LES in the atmospheric flow community. Despite being fundamental to CFD studies, mesh generation still lacks a unified framework, and crucial mesh-related information remain largely absent from the literature (Pantusheva et al. 2025).

In the case of the CEDVAL A1-1 wind-tunnel dataset, several LES studies (e.g., Cotteleer et al., 2023; Ai and Mak, 2015) report mesh cell counts, coarsening strategies, and y+ values, but generally omit key information needed to evaluate turbulence and flow-resolution quality. Sivaraman et al. (2025) provide a more complete methodology based on Pope's criteria and ensuring that the SGS model operates within its validity range. Building on Pantusheva et al. (2025), who initiated a systematic approach for urban-mesh generation, this work evaluates mesh-quality metrics for atmospheric flows in built-up areas and proposes an automated mesh-convergence workflow for LES.

2 METHODS

The truly neutral filtered LES incompressible Navier-Stokes equations without the Coriolis force are considered. They are solved using the incompressible solver of the highly parallel YALES2 platform (Moureau et al., 2010). It relies on 4th order explicit time integration and 4th order central finite-volume schemes and the use of unstructured dual-meshes.

Mesh adaptation workflow

The automated mesh convergence workflow is based on two criteria:

$$Re_{\Delta}^{\langle u \rangle} = \frac{c\Delta^3 \| \frac{\partial^2 \langle u \rangle}{\partial x_i^2} \|_{L2}}{\nu + \nu_T} \quad \text{and} \quad L/\Delta \tag{1}$$

where ν_T is the turbulent kinematic viscosity acting on the mean field in LES, Δ the local cell size, c a constant depending on the dimension of the problem ($c = 1/5$ in 3D) and L the integral length scale.

The first criterion is a Reynolds number based on the mean velocity error which controls the mean flow independence to meshes composed of isotropic tetrahedra (Lam et al., 2025). The second criterion monitors the resolution of turbulent structures using the ratio of integral length scale L over the local cell size Δ (Barbera et al. personal communication). This ensures that the cell size lies within the inertial subrange and provides explicit control over the contribution of the SGS model. For prescribed values of $Re_{\Delta}^{\langle u \rangle}$ and L/Δ, two local target cell sizes are computed: $\Delta^{\langle u \rangle}$ and Δ^{sgs}, respectively. The final target cell size Δ^t is then defined as $\Delta^t = \min(\Delta^{\langle u \rangle}, \Delta^{sgs})$.

The workflow starts from a user-defined initial mesh and follows an iterative sequence of LES computations and mesh-adaptation steps. Convergence is reached when the total number of elements varies by less than 10% between two successive iterations. The resulting mesh is then referred to as the converged mesh, indicating that the prescribed convergence criteria are satisfied.

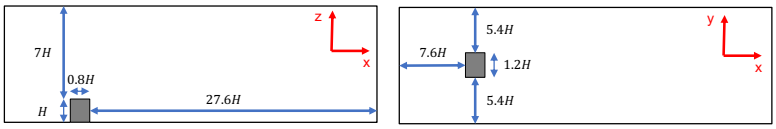

Figure 1: Side (left) and top (right) views of the computational domain, based on Cotteleer et al. (2023).

Numerical setup

The CEDVAL A1-1 wind-tunnel experiment (Leitl and Schatzmann, 2010), involving a truly neutral turbulent flow around an isolated obstacle, is investigated. The numerical domain is shown in Fig. 1, with a characteristic height $H = 0.125\,\mathrm{m}$ and designed by Cotteleer et al. (2023) according to best practices and guidelines. Slip boundary conditions are applied at the upper and spanwise boundaries. A logarithmic law-of-the-wall is imposed at the ground and obstacle surfaces. The inlet boundary condition consists of the superposition of a static mean profile used by Cotteleer et al. (2023), and a time-varying fluctuating profile obtained from Homogeneous Isotropic Turbulence (HIT). This HIT is parameterized using the experimental turbulent length scale l_e and the turbulent kinetic energy profile from Cotteleer et al. (2023), assuming $\sqrt{k} \cong \sigma_u$.

A static mesh (ST) is used as a reference, following Cotteleer et al. (2023) and Ai and Mak (2015), with obstacle-adjacent cell sizes ensuring $y^+ \leq 10$. The Automatic Mesh Convergence (AMC) strategy is applied starting from a coarse initial mesh and using the parameters $Re_{\Delta}^{\langle u \rangle} = 20$ and $L/\Delta = 5$. The characteristics of the ST mesh, as well as those of the initial and converged AMC meshes, are summarized in Tab. 1 and illustrated in Fig. 2.

Table 1: Mesh characteristics (* Number of elements and nodes between $x = 0.0\,\mathrm{m}$ and $x = 2.0\,\mathrm{m}$)

Mesh name	Δ_{obstacle} [m]	Δ_{surface} [m]	$\Delta_{\text{background}}$ [m]	Growth rate	N^*_{elem}	N^*_{node}
ST	0.00125	0.00125	0.02	1.2	6.01×10^7	1.12×10^7
AMC - initial	0.04	0.04	0.04	-	4.00×10^4	7.47×10^4
AMC - final	0.0002 - 0.024	0.0002 - 0.085	0.00037 - 0.091	1.3	7.0×10^6	1.5×10^6

Figure 2: Slice along the y-axis of the ST (left), initial AMC (middle) and final AMC (right) meshes

3 RESULTS AND DISCUSSION

Time-averaged streamwise velocity profiles for different streamwise positions are shown in Fig. 3. Both the ST mesh and the converged AMC mesh show good agreement with the experimental measurements. However, results obtained with the AMC mesh are less accurate in the wake of the obstacle, particularly in the transition region between the turbulent flow and the recirculation zone. This behavior is attributed to the chosen parameter $L/\Delta = 5$ which is not restrictive enough to capture the flow structures in this region. The local cell size being around $l_e/4$ in this region, i.e. four times larger than the ST mesh, the turbulence may neither be homogeneous nor isotropic at this scale, leaving the SGS models out of their validity range. Discrepancies with respect to experimental measurements appear above the height of the obstacle for both meshes. The flow dynamics is directly impacted by the turbulent inlet in this area. The reliability of the choice of HIT-induced fluctuations is questionable and will be the subject of further investigation.

Figure 3 also provides streamwise velocity RMS profiles for the same streamwise positions. Both meshes are in good agreement with the experimental data. Nevertheless, the highest RMS values are better captured with the ST mesh, for which the near-wall region on the obstacle is more accurately resolved. The lower accuracy of the converged AMC mesh is mainly due to the mean field criterion $Re_\Delta^{\langle u \rangle} = 20$ which is not sufficiently restrictive in this region, whereas values close to $Re_\Delta^{\langle u \rangle} = 5$ are obtained on top of the obstacle for the ST mesh (maps not shown here for the sake

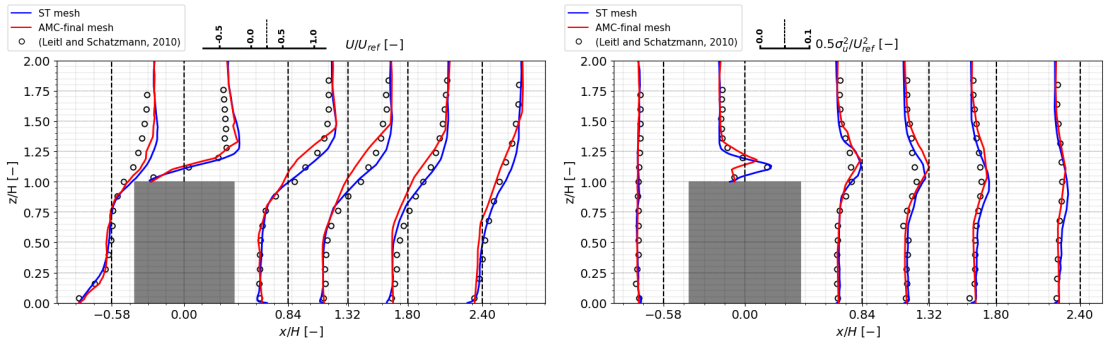

Figure 3: Mean (left) and RMS (right) streamwise velocity profiles in the $y = 0$ center plane along different streamwise positions.

of brevity).

For a characteristic time $\tau = 36H/U_{ref}$, the simulation costs $2.9\,\mathrm{kCPUh}$ for the final AMC mesh, 50% less than the ST mesh with $4.5\,\mathrm{kCPUh}$. Despite having a smaller convective time step induced by a lower smallest cell size, the final AMC mesh cost remains lower because of fewer mesh elements. This improved cost reveals the potential of the AMC methodology to optimize the precision-over-cost ratio, crucial in CFD simulations.

4 CONCLUSION

An original criteria-based methodology has been proposed to automatically converge meshes for atmospheric flows in complex environment. Applied to a turbulent flow around an isolated obstacle, it allowed to retrieve the mean and RMS velocity characteristics. In addition to the mesh convergence methodology, these criteria allow quantifying the resolution of a given mesh and could be provided as intrinsic mesh characteristics. Future works imply the determination of a reference set of criteria values that allow a faithful description of the flow, especially near the obstacle surface and in its wake. The methodology could then be applied to more realistic cases with pollutant dispersion, where an accurate capture of high-RMS regions is essential.

5 ACKNOWLEDGMENTS

The authors thank R. Barbera and G. Balarac for their valuable advice on the numerical methodology. This project was provided with computer and storage resources by GENCI at CINES thanks to the grant 2025-A0182A11335 on the supercomputer Adastra's the GENOA partition and computing resources of CRIANN (Normandy, France) under the allocation 2012006.

REFERENCES

Moureau, V., Domingo, P., Vervisch, L., 2010. Design of a massively parallel CFD code for complex geometries. C. R. Méca, 339(2-3), 141-148. https://doi.org/10.1016/j.crme.2010.12.001

Lam, H., Berthelon, T., Balarac, G., 2025. Non-dimensional meshing criterion of mean flow field discretization for RANS and LES. Comput. Fluids., 291, 106572. https://doi.org/10.1016/j.compfluid.2025.106572

Pantusheva, M., Mitkov, R., Hristov, P. O., Petrova-Antonova, D., 2022. Air Pollution Dispersion Modelling in Urban Environment Using CFD : A Systematic Review. Atmos., 13(10), 1640. https://doi.org/10.3390/atmos13101640

Pantusheva, M., Petrova-Antonova, D., Naserentin, V., Mitkov, R., Spaias, G., Logg, A., 2025. Towards a Comprehensive Workflow for Mesh Generation in Urban Wind Engineering using CFD. J. Phys. Conf. Ser., 3027(1), 012079. https://doi.org/10.1088/1742-6596/3027/1/012079

Tominaga, Y., 2024. CFD simulations of turbulent flow and dispersion in built environment : A perspective review. J. Wind Eng. Ind. Aerodyn. 249, 105741. https://doi.org/10.1016/j.jweia.2024.105741

Cotteleer, L., Longo, R., Debaste, F., Parente, A., 2023. Flow-based stress-blended eddy simulation : A local RANS/LES turbulence model for urban flow CFD simulations. Results Eng., 21, 101679. https://doi.org/10.1016/j.rineng.2023.101679

Ai, Z., Mak, C., 2015. Large-eddy Simulation of flow and dispersion around an isolated building : Analysis of influencing factors. Comput. Fluids., 118, 89-100. https://doi.org/10.1016/j.compfluid.2015.06.006

Leitl, B., Schatzmann, M., 2010. Cedval at Hamburg university, https://www.mi.uni-hamburg.de/en/arbeitsgruppen/windkanallabor/data-sets.html (accessed 27 November 2025)

Barbera, R., personal communication. Adaptation de maillage anisotrope et schémas numériques pour la simulation aux grandes échelles des interfaces. Ph. D. Thesis. Université Grenoble Alpes.